

Synthesis and Structures of Gallium Amido Imido Phenyl Clusters (PhGa)₄(NHⁱBu)₄(NⁱBu)₂ and (PhGa)₇(NHMe)₄(NMe)₅

Bing Luo and Wayne L. Gladfelter*

Department of Chemistry, University of Minnesota, Minneapolis, Minnesota 55455

Received February 1, 2002

The phenylgallium-containing clusters constructed with bridging imido and amido ligands, (PhGa)₄(NHⁱBu)₄(NⁱBu)₂ (**1**) (51% yield) and (PhGa)₇(NHMe)₄(NMe)₅ (**2**) (31% yield), were synthesized from the room-temperature reactions of bis(dimethylamido)phenylgallium, [PhGa(NMe₂)₂]₂, with isobutylamine and methylamine, respectively. The reaction of [PhGa(NMe₂)₂]₂ in refluxing isobutylamine (85 °C) afforded (Ph₂GaNHⁱBu)₂ as one of the products, while the reaction of [PhGa(NMe₂)₂]₂ with methylamine at 150 °C afforded compound **2** in only 9% yield. Compound **1** possessed an adamantane-like Ga₄N₆ core, whereas compound **2** had a novel Ga₇N₉ core constructed with both chair- and boat-shaped Ga₃N₃ rings. The presence of several isomers of compounds **1** and **2** in solution is discussed along the structural similarities with other known gallium–nitrogen clusters and with gallium nitride.

Introduction

There has been much work in synthesizing nanocrystalline GaN that would lead to a systematic increase in the band gap of this σ -delocalized electronic structure.^{1–12} Although some size control has been achieved,^{9–12} these methods produce a wide distribution in particle sizes making meaningful measurements of optical properties difficult. An alternative method is to synthesize ever-larger, molecular clusters in which R₃Ga and R₃N moieties form a framework of Ga–N bonds.

We recently reported the structural characterization of two gallium–nitrogen clusters, (PhGaNPh)₄ and (PhGaNMe)₇.¹³ The formation of these compounds, several known tetramers,^{14–16} and a hexamer [MeGaN(4-C₆H₅F)]₆¹⁷ was facilitated by hydrocarbon elimination in the reactions of triorganylgallium with aniline or primary amines at elevated temperatures. This type of reaction has also produced a gallium amido imido compound, (MeGaNMe)₆(Me₂-GaNHMe)₂.¹⁸ In a similar reaction, another hexamer (MeGa-NⁱBu)₆ was synthesized from pyrolysis of [Me₂GaN(ⁱBu)-(SnMe₃)₂]₂.¹⁹ A transamination route involving the reactions of R₃Ga(NMe₂)₂ with primary amines is reported here and represents a new route leading to gallium–nitrogen clusters. It allows the systematic variation in ligand size that may control the cluster nuclearity. An excellent review of gallium amides has recently appeared.²⁰

Experimental Section

Materials and General Procedures. All chemicals were purchased from Aldrich. Anhydrous methylamine was used as received.

* To whom correspondence should be addressed. E-mail: gladfelter@chem.umn.edu.

- (1) Morkoc, H.; Mohammad, S. N. *Science* **1995**, *267*, 51–55.
- (2) Hwang, J.-W.; Campbell, J. P.; Kozubowski, J.; Hanson, S. A.; Evans, J. F.; Gladfelter, W. L. *Chem. Mater.* **1995**, *7*, 517.
- (3) Goodwin, T. J.; Leppert, V. J.; Smith, C. A.; Risbud, S. H.; Niemeyer, M.; Power, P. P.; Lee, H. W. H.; Hrubesh, L. W. *Appl. Phys. Lett.* **1996**, *69*, 322–324.
- (4) Janik, J. F.; Wells, R. L. *Chem. Mater.* **1996**, *8*, 2708–2711.
- (5) Coffey, J. L.; Johnson, M. A.; Zhang, L.; Wells, R. L.; Janik, J. F. *Chem. Mater.* **1997**, *9*, 2671–2673.
- (6) Frank, A. C.; Stowasser, F.; Sussek, H.; Pritzkow, H.; Miskys, C. R.; Ambacher, O.; Giersig, M.; Fischer, R. A. *J. Am. Chem. Soc.* **1998**, *120*, 3512–3513.
- (7) McMurran, J.; Kouvetakis, J.; Nesting, D. C.; Smith, D. J.; Hubbard, J. L. *J. Am. Chem. Soc.* **1998**, *120*, 5233–5237.
- (8) Jegier, J. A.; McKernan, S.; Gladfelter, W. L. *Chem. Mater.* **1998**, *10*, 2041.
- (9) Frank, A. C.; Fischer, R. A. *Adv. Mater.* **1998**, *10*, 961–964.
- (10) Micic, O. I.; Ahrenkiel, S. P.; Bertram, D.; Nozik, A. J. *Appl. Phys. Lett.* **1999**, *75*, 478–480.
- (11) Jegier, J. A.; McKernan, S.; Purdy, A. P.; Gladfelter, W. L. *Chem. Mater.* **2000**, *12*, 1003–1010.
- (12) Manz, A.; Birkner, A.; Kolbe, M.; Fischer, R. A. *Adv. Mater.* **2000**, *12*, 569–573.

- (13) Luo, B.; Gladfelter, W. L. *Inorg. Chem.* **2002**, *41*, 590–597.
- (14) Belgardt, T.; Roeksy, H. W. *Angew. Chem., Int. Ed. Engl.* **1993**, *32*, 1056–1058.
- (15) Cordeddu, F.; Hausen, H.-D.; Weidlein, J. Z. *Anorg. Allg. Chem.* **1996**, *622*, 573–578.
- (16) Kühner, S.; Kuhnle, R.; Hausen, H.-D.; Weidlein, J. Z. *Anorg. Allg. Chem.* **1997**, *623*, 25.
- (17) Schnitter, C.; Waezsada, S. D.; Roeksy, H. W.; Teichert, M.; Usón I., Parisini, E. *Organometallics* **1997**, *16*, 1197–1202.
- (18) Amirkhalili, S.; Hitchcock, P. B.; Smith, J. D. *J. Chem. Soc., Dalton Trans.* **1979**, 1206–1212.
- (19) Schmid, K.; Niemeyer, M.; Weidlein, J. Z. *Anorg. Allg. Chem.* **1999**, *625*, 186–188.

Isobutylamine was distilled over calcium hydride under nitrogen. Bis(dimethylamido)phenylgallium, $[\text{PhGa}(\text{NMe}_2)_2]_2$, was synthesized as previously reported.²¹ Diethyl ether, pentane, hexanes, and toluene were predried over calcium hydride and freshly distilled over sodium/benzophenone under nitrogen. Benzene- d_6 and toluene- d_8 were distilled over calcium hydride under nitrogen. All experiments were conducted under an oxygen-free, dry-nitrogen atmosphere using standard Schlenk and glovebox techniques.

Room-temperature 1-D and 2-D ^1H NMR and ^{13}C NMR spectra were obtained in a toluene- d_8 solution (for compound **1**) or a benzene- d_6 solution (for compound **2**) on a Varian INOVA 500 spectrometer. Additional 1-D and 2-D spectra of saturated toluene- d_8 solutions of compound **2** at 25 °C were acquired at 800 MHz (^1H resonance frequency) on a Varian INOVA spectrometer using a 5 mm HCN probe. Variable-temperature ^1H NMR spectra were recorded in a toluene- d_8 solution on a Varian INOVA 300 spectrometer. The ^1H NMR spectra were referenced to the sharp singlet from silicone grease at δ 0.29 in benzene- d_6 or δ 0.27 in toluene- d_8 . The ^{13}C NMR spectra were referenced to the carbons of benzene- d_6 (δ 128.39) or toluene- d_8 (δ 137.86). The IR spectra of KBr pellets were recorded on a Nicolet MAGNA-IR 560 spectrometer. Chemical ionization mass spectra were acquired on a Finnigan Mat 95 spectrometer using a direct insertion probe. The samples were evaporated at temperatures ranging from 25 to 340 °C, and the ionization gas mixture was methane with 4% ammonia. Melting points were obtained in sealed, nitrogen-filled capillaries and were uncorrected. Elemental analyses were obtained from Schwarzkopf Microanalytical Laboratories, Woodside, NY, or Desert Analytics, Tucson, AZ.

Synthesis of $(\text{PhGa})_4(\text{NH}^i\text{Bu})_4(\text{N}^t\text{Bu})_2$ (1**).** Isobutylamine (3 mL) was added to a flask containing $[\text{PhGa}(\text{NMe}_2)_2]_2$ (1.00 g, 2.13 mmol) at room temperature. Gas evolution was observed immediately, and a clear solution formed. The solution was stirred for 2 h, and volatiles were removed under vacuum leaving a glassy, colorless solid. Pentane (10 mL) and toluene (2 mL) were added, and the solution was stored at -20 °C. After 1 week, colorless blocks of compound **1** containing solvents crystallized. From these a crystal suitable for single-crystal XRD analysis was chosen. A solvent-free sample (0.55 g, 51% yield) was obtained as a white powder after the crystals were heated at 50 °C under vacuum. Mp: 98–100 °C (melt remained a liquid upon cooling to room temperature). CI MS (m/e) [assignment, % relative intensity]: 1036 $[(\text{M} + \text{NH}_4)^+, 0.7]$, 1014 $[(\text{M} - \text{Ph} + \text{H}_2\text{N}^t\text{Bu})^+, 6.0]$, 941 $[(\text{M} - \text{Ph})^+, 2.4]$, 890 $[(\text{PhGa}^i\text{N}^t\text{Bu})_4 + \text{NH}_4]^+, 3.9]$, 873 $[(\text{PhGa}^i\text{N}^t\text{Bu})_4 + \text{H}]^+, 100]$, 795 $[(\text{PhGa}^i\text{N}^t\text{Bu})_4 - \text{Ph}]^+, 16]$, 593 $[(\text{Ph}_2\text{GaNH}^i\text{Bu})_2 + \text{H}]^+, 4.0]$, 532 $[(\text{Ph}_2\text{GaNH}^i\text{Bu})_2 - \text{Ph} + \text{NH}_3]^+, 14]$, 74 $[(\text{BuNH}_3)^+, 93]$. IR (cm^{-1}): ν_{NH} , 3281 and 3269. ^1H NMR (21 °C, 500 MHz, toluene- d_8): more than 40 overlapping multiplets were present in the range of δ 0.3–4.0 for the N^tBu and $\text{N}(\text{H})^i\text{Bu}$ groups. The resonances attributed to the *meta* and *para* phenyl hydrogens appeared at δ 6.9 to 7.5, while 10 doublets ($J = 7$ Hz) assigned to the *ortho* hydrogens were observed at δ 7.61, 7.63, 7.70, 7.75, 7.78, 7.81, 7.87, 7.95, 7.96 and 8.00. A 500 MHz ^1H NMR spectrum is available in the Supporting Information. The ^1H NMR spectra collected from -60 to $+95$ °C were essentially the same as the room-temperature spectrum. ^{13}C NMR (21 °C, ^1H -decoupled, 500 MHz, toluene- d_8): δ 14.67, 23.19, 31.90, 31.93, 32.01, 32.04, 32.11, 32.14, 32.18, 32.33, 32.52, 32.54, 32.62, 32.64, 32.65, 32.69, 32.81, 34.92, 35.14, 35.20, 35.28, 35.31, 36.50, 36.56, 36.80. and 37.35 for $\text{NCH}_2\text{CH}(\text{CH}_3)_2$ and $\text{NHCH}_2\text{CH}(\text{CH}_3)_2$; 52.83,

52.87, 53.92, 54.03, 55.56, 55.63, 55.73, 57.34, 60.21, 60.36, and 60.57 for $\text{NCH}_2\text{CH}(\text{CH}_3)_2$ and $\text{NHCH}_2\text{CH}(\text{CH}_3)_2$. The phenyl carbons were overlapping with the intense resonances from the solvent and not distinguished.

Pyrolysis of Compound 1. A crystalline sample of **1** (0.75 g) was heated at 150 °C for 2 h. It melted at ca. 100 °C and started to react as evidenced by the formation of volatiles collected in a trap at -196 °C. At the end of the reaction, a glassy solid was obtained at room temperature. Pentane (10 mL) was added resulting in the formation of a colorless solution. After the solution was stored at -20 °C for 2 days, a colorless crystalline solid formed (0.12 g, 14% yield based on gallium) which was characterized as $[\text{Ph}_2\text{Ga}(\text{H})^i\text{Bu}]_2$ by comparing its IR and ^1H NMR spectra with those of the authentic sample.¹³ The remaining compounds in the solution formed a glassy solid upon pentane evaporation, and the ^1H NMR spectrum showed a complex pattern. The liquid collected (ca. 0.08 g) in the trap during pyrolysis was a mixture of $\text{H}_2\text{N}^t\text{Bu}$, toluene, and pentane as determined by the ^1H NMR spectroscopy.

In another experiment, neat compound **1** (0.50 g) was heated to 300 °C within a period of 0.5 h. Initially a colorless, sticky liquid formed, and it turned into black after 0.5 h. A metal mirror was observed when the products were cooled to room temperature, indicative of the formation of gallium metal.

Reaction of $[\text{PhGa}(\text{NMe}_2)_2]_2$ in Refluxing $\text{H}_2\text{N}^t\text{Bu}$. Isobutylamine (2.00 mL, 1.47 g, 20.1 mmol) was added to a flask containing $[\text{PhGa}(\text{NMe}_2)_2]_2$ (0.800 g, 1.70 mmol) at room temperature. Gas evolution was observed immediately, and a colorless solution formed. The solution was heated to reflux (85 °C) for 20 h. Volatiles were removed under vacuum, and a colorless, sticky solid remained. Pentane (10 mL) was added, and the mixture was filtered to separate a small amount of a white precipitate from a clear filtrate. The filtrate was stored at 0 °C for several days, and colorless blocks were isolated (0.35 g, 35% yield based on gallium) and characterized as $[\text{Ph}_2\text{Ga}(\text{H})^i\text{Bu}]_2$ by comparing its IR and ^1H NMR spectra with those of the authentic sample.¹³

Synthesis of $(\text{PhGa})_7(\text{NHMe})_4(\text{NMe})_5$ (2**).** Methylamine (3 mL) was condensed into a gauged flask at -196 °C and was transferred through a cannula into a solution of $[\text{PhGa}(\text{NMe}_2)_2]_2$ (1.32 g, 1.81 mmol) in 20 mL of toluene at -78 °C. A colorless solution was obtained at low temperatures. After the solution was allowed to warm to room temperature and stirred for 1 h, it became cloudy. Stirring was continued for another 15 h, and volatiles were removed in a vacuum affording a colorless glassy solid. Toluene (15 mL) was added, and the resulting slurry was filtered to separate 0.15 g of an unidentified white solid and a colorless filtrate. Pentane (20 mL) was added to the filtrate, and the solution was stored at -20 °C. After several days colorless crystals of compound **2** were isolated, and some block-shaped crystals were suitable for the single-crystal XRD analysis. A solvent-free sample (0.32 g, 31% yield) was obtained as a white powder after the crystals were heated at 50 °C under vacuum. Mp: 173 °C (decomposed to a glassy solid). In the chemical-ionization mass spectral experiment, two maxima, which appeared 4 and 5.6 min after the sample injection, were found in the ion abundance curve and corresponded to the evaporating temperatures of ca. 250 and 340 °C, respectively. Two spectra were collected corresponding to the two maxima. The first spectrum exhibited major m/e peaks below 160 and no peaks above m/e 400 were present. The following data were obtained from the second spectrum suggesting the formation of the heptameric $(\text{PhGaNMe})_7$ due to the decomposition of **2**. CI MS (m/e) [assignment, % relative intensity]: 1231 $[(\text{PhGaNMe})_7^+, 5.6]$, 1218 $[(\text{PhGaNMe})_7 - \text{Me} + 2\text{H}]^+, 1.0]$, 1154 $[(\text{PhGaNMe})_7 - \text{Ph}]^+, 3.4]$, 78 $[(\text{C}_6\text{H}_6)^+, 100]$. IR (cm^{-1}): ν_{NH} , 3265. Anal. Calcd for $\text{C}_{51}\text{H}_{66}\text{Ga}_7\text{N}_9$: C, 47.37; H,

(20) Carmalt, C. J. *Coord. Chem. Rev.* **2001**, 223, 217–264.

(21) Jegier, J. A.; Luo, B.; Buss, C. E.; Gladfelter, W. L. *Inorg. Chem.* **2001**, 40, 2017–2021.

5.14; N, 9.75. Found: C, 47.55; H, 5.46; N, 7.24. ^1H NMR (25 °C, 800 MHz, toluene- d_8): δ 0.782 (d, 6.4 Hz, NHCH_3), 0.880 (q, 7.2 Hz, NH), 0.882 (q, 7.2 Hz, NH), 1.065 (q, 6.4 Hz, NH), 1.10 (q, 6.4 Hz, NH), 1.19 (q, 7.2 Hz, NH), 1.26 (q, 7.2 Hz, NH), 1.27 (d, 7.2 Hz, NHCH_3), 1.38 (q, 7.2 Hz, NH), 1.54 (q, 6.4 Hz, NH), 1.92 (d, 6.4 Hz, NHCH_3), 2.08 (d, 7.2 Hz, NHCH_3), 2.19 (d, 6.4 Hz, NHCH_3), 2.23 (d, 7.2 Hz, NHCH_3), 2.27 (d, 6.4 Hz, NHCH_3), 2.28 (d, 6.4 Hz, NHCH_3), 2.30 (d, 6.4 Hz, NHCH_3), 2.32 (d, 6.4 Hz, NHCH_3), 2.36 (d, 6.4 Hz, NHCH_3), 2.42 (d, 6.4 Hz, NHCH_3), 2.42 (s, NMe), 2.63 (q, 6.4 Hz, NH), 2.65 (s, NMe), 2.70 (q, 6.4 Hz, NMe), 2.92 (s, NMe), 2.94 (s, NMe), 3.07 (s, NMe), 3.08 (s, NMe), 3.13 (s, NMe), 3.14 (s, NMe), 3.46 (s, NMe), 3.47 (s, NMe), 3.48 (s, NMe), 3.49 (s, NMe), 3.52 (s, NMe), 3.54 (s, NMe), 6.9–8.2 (m, Ph). ^{13}C NMR (21 °C, ^1H -decoupled, 500 MHz, benzene- d_6): δ 32.52, 32.56, 32.75, 32.81, 32.89, 32.92, 32.95, 33.13, 33.44, 33.46, 33.60, and 34.14 for NHCH_3 ; 38.92, 39.02, 39.38, 39.82, 40.03, 40.20, 40.33, 41.03, 41.20, 41.31, and 41.78 for NCH_3 ; 126.03, 128.90, 128.97, 129.10, 129.22, 129.66, 137.37, 137.62, 137.72, 137.75, 137.77, 137.82, 138.02, 138.05, 138.11, 138.18, 138.22, 138.27, 139.16, and 139.26 for phenyl carbons.

Isolation of 2 from the Reaction of $[\text{PhGa}(\text{NMe}_2)_2]_2$ with H_2NMe at 150 °C. Methylamine (15 mL) was condensed and transferred into an autoclave containing $[\text{PhGa}(\text{NMe}_2)_2]_2$ (3.00 g, 6.40 mmol) at low temperatures. The autoclave was heated to 150 °C for 15 h, and the reaction pressure was ca. 40 psi. At the end of the reaction, the excess methylamine was released and a white powder (1.60 g) was collected. The solid was dissolved in 50 mL of toluene, and filtration removed 0.28 g of an unidentified white solid that exhibited C–H and N–H absorptions at 2777–3184 cm^{-1} in the infrared spectrum. Pentane (20 mL) was added to the filtrate, and the solution was stored at –20 °C. After 1 week, compound **2** was isolated (0.20 g, 8.5% yield).

X-ray Data Collection, Structure Solution, and Refinement. Suitable crystals of compounds **1** and **2** were selected and mounted on top of glass fibers under nitrogen. Both data collections were conducted on a Siemens SMART system. In each experiment, an initial set of cell constants was calculated from reflections harvested from three sets of 20 frames. These sets of frames were oriented such that orthogonal wedges of reciprocal space were surveyed. A randomly oriented region of reciprocal space was surveyed to the extent of 1.3 hemispheres to a resolution of 0.77 Å for **1** and 0.84 Å for **2**. Three major swaths of frames were collected with 0.30° steps in ω . The final cell constants were calculated from a set of 5484 reflections for compound **1** and 6247 reflections for **2**.

The space group of $P\bar{1}$ for compounds **1** and **2** was determined on the basis of the lack of systematic absences and on the intensity statistics. A successful direct-methods solution was applied to both structures that provided most non-hydrogen atoms from the E -maps. Several full-matrix, least-squares/difference Fourier cycles were performed to locate the remainder of the non-hydrogen atoms. Except for the disordered C(43D) having a 19% occupancy ratio in the structure of **2**, all non-hydrogen atoms were refined with anisotropic displacement parameters. H(2N) and H(4N) in the structure of **1** were found from the difference Fourier maps, and all the other hydrogen atoms in both structures were placed in ideal positions. All hydrogen atoms were refined isotropically or as riding atoms with relative isotropic displacement parameters.

In the structure of **1** the hydrogen atoms on N(1) and N(3) were not found from the Fourier maps, but N(1) and N(3) were determined to be amido nitrogen atoms on the basis of a comparison of the relevant Ga–N bond lengths and Ga–N–Ga bond angles with those for other nitrogen atoms (see Table 2 and the discussion below). Similarly, N(1), N(2), N(8), and N(9) in the structure of **2**

Table 1. Crystallographic Data for Compounds **1** and **2**^a

param	(PhGa) ₄ (NH ^t Bu) ₄ (N ⁱ Bu) ₂ (1)	(PhGa) ₇ (NHMe) ₄ (NMe) ₅ (2)
fw	1018.04	646.58
space group	$P\bar{1}$	$P\bar{1}$
<i>a</i> , Å	12.8604(8)	12.4674(13)
<i>b</i> , Å	12.9059(8)	15.3881(16)
<i>c</i> , Å	19.0549(11)	18.3660(19)
α , deg	75.6740(10)	95.795(2)
β , deg	81.8910(10)	109.347(2)
γ , deg	60.9670(10)	113.013(2)
<i>V</i> , Å ³	2678.4(3)	2950.2(5)
<i>Z</i>	2	2
<i>T</i> , °C	–100	–100
λ , Å	0.710 73	0.710 73
ρ_{calcd} , g cm ^{–3}	1.262	1.456
μ , cm ^{–1}	20.25	31.86
<i>R</i> ₁ [<i>I</i> > 2 σ (<i>I</i>)], w <i>R</i> ₂ (all data) ^b	0.0508, 0.1119	0.0417, 0.1056

^a The formulas, formula weights, and calculated densities excluded the solvents that were present in the crystal lattices and were not refined. ^b $R_1 = \Sigma||F_o| - |F_c||/\Sigma|F_o|$ and $wR_2 = \{\Sigma[w(F_o^2 - F_c^2)^2]/\Sigma[w(F_o^2)^2]\}^{1/2}$, where $w = 1/[\sigma^2(F_o^2) + (aP)^2 + (bP)]$, $P = (F_o^2 + 2F_c^2)/3$, and *a* and *b* are constants given in the Supporting Information.

were determined to be amido nitrogens. The refinement for hydrogens supported these assignments; except for the disordered H(1N) atoms in both structures, the refinement for H(3N) in **1** and H(2N), H(8N), and H(9N) in **2** gave reasonable isotropic displacement parameters.

In the structure of **1**, the two isobutylamido groups containing N(1), C(25)–C(28) and N(3), and C(33)–C(36) were disordered over two positions with the occupancy ratios being 55:45 and 66:34, respectively. In the structure of **2**, four phenyl groups, C(1)–C(6) (site occupancy ratio, 64:36), C(7)–C(12) (58:42), C(19)–C(24) (52:48), and C(25)–C(30) (82:18), and an amido group, N(1) and C(43) (81:19), were found to be disordered over two positions for each.

In both structures, individual solvent molecules in the lattices could not be located. The data sets were corrected for the solvents using the PLATON/SQUEEZE program, and the refinements using the corrected data sets improved the overall structures and *R*₁ values by 1.3% for **1** and 1.5% for **2**, respectively. The experimental conditions and unit cell information are summarized in Table 1. All calculations were performed using SGI INDY R4400-SC or Pentium computers and the SHELXTL V5.0 suite of programs.

Results

Synthesis and Structural Determination of (PhGa)₄(NH^tBu)₄(NⁱBu)₂ (1**) and (PhGa)₇(NHMe)₄(NMe)₅ (**2**).** Compounds **1** and **2** were synthesized from the reactions of $[\text{PhGa}(\text{NMe}_2)_2]_2$ in neat, excess $\text{H}_2\text{N}^i\text{Bu}$ and in a toluene solution of excess H_2NMe , respectively (Scheme 1). Both reactions occurred at room temperature, and the crude products were colorless, glassy solids. In the H_2NMe reaction, a small amount of unidentified white solid, insoluble in toluene, also formed. Compounds **1** and **2** crystallized from mixed toluene and pentane solutions, and the solvent-free samples of **1** (51% yield based on gallium) and **2** (31% yield) were obtained as white powders. In repeated attempts for elemental analysis, the determined C, H, and N percentages of compound **1** were below the calculated values, possibly due to formation of involatiles in the elemental analysis process. The results of the C and H analysis for compound **2** were satisfactory, but the nitrogen percentage was 2% below the calculated value.

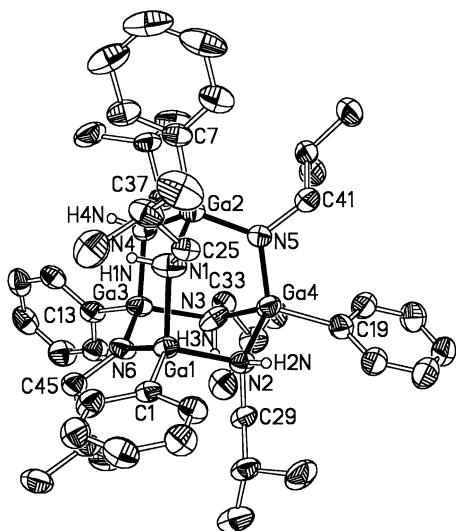
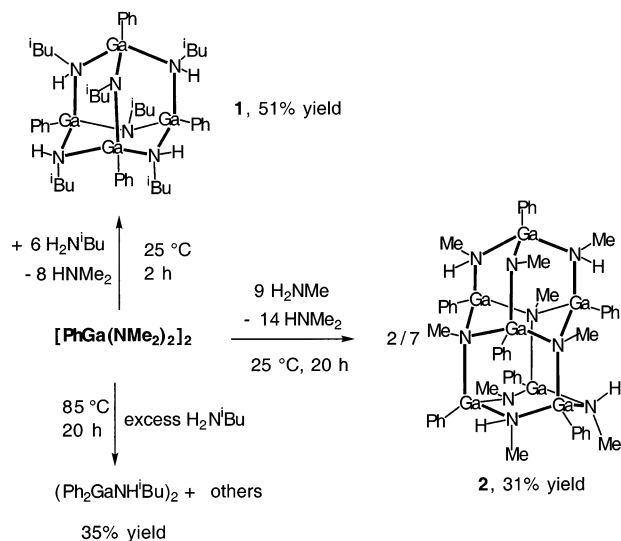


Figure 1. Molecular structure and atom-labeling scheme for $(\text{PhGa})_4(\text{NH}^i\text{-Bu})_4(\text{N}^t\text{-Bu})_2$ (**1**). Atoms are shown at the 30% probability level. Disordered atoms and all hydrogens except those on nitrogens are omitted.

Scheme 1



The molecular structures of compounds **1** and **2** are shown in Figures 1 and 2, respectively, and selected bond lengths and angles are listed in Tables 2 and 3. Four chair-shaped Ga_3N_3 rings comprise the adamantane-like Ga_4N_6 core in the structure of compound **1**. The imido nitrogen atoms N(5) and N(6) were readily recognized from their trigonal planar geometry and the shorter Ga–N bonds [1.851(3)–1.855(4) Å] than others [2.004(4)–2.019(4) Å] in the structure. Gallium compounds with three-coordinate, bridging imido groups are uncommon. A hydrazide derivative containing such imido nitrogen atoms,²² $\text{Ga}_4(\text{NHNMe}_2)_8(\text{NNMe}_2)_2$, had the corresponding Ga–N bond lengths of 1.847(3) and 1.860(3) Å and trigonal planar geometries of the imido nitrogens. The N–Ga–N bond angles in the structure of **1** varied from 97.85(15) to 112.12(15)°, and the Ga–N–Ga bond angles, from 115.06(7) to 120.63(18)°. An examination of the previously reported group 13 metal adamantane-like struc-

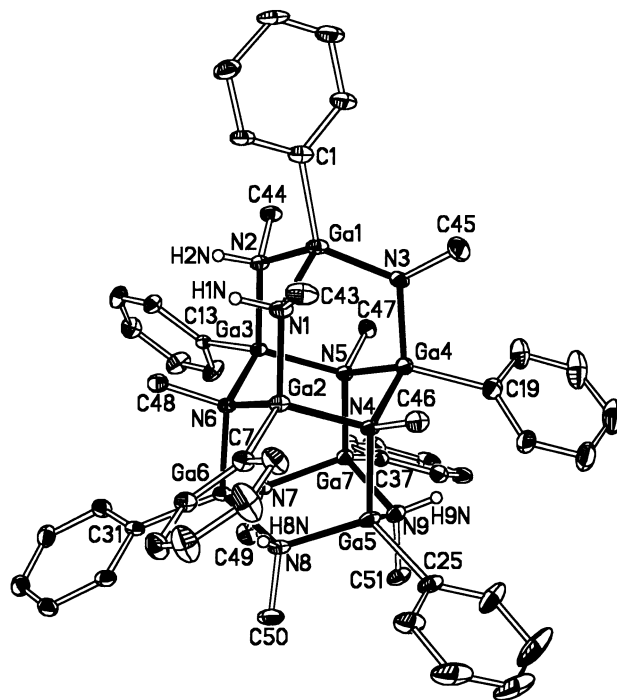


Figure 2. Molecular structure and atom-labeling scheme for $(\text{PhGa})_7-(\text{NHMe})_4(\text{NMe})_5$ (**2**). Atoms are shown at the 15% probability level. Disordered atoms and all hydrogens except those on nitrogens are omitted.

Table 2. Selected Bond Lengths (Å) and Angles (deg) for $(\text{PhGa})_4(\text{NH}^i\text{-Bu})_4(\text{N}^t\text{-Bu})_2$ (**1**)

Ga(1)–C(1)	1.984(4)	Ga(3)–C(13)	1.983(4)
Ga(1)–N(1)	2.008(3)	Ga(3)–N(3)	2.019(4)
Ga(1)–N(2)	2.004(4)	Ga(3)–N(4)	2.007(4)
Ga(1)–N(6)	1.851(3)	Ga(3)–N(6)	1.853(3)
Ga(2)–C(7)	1.986(4)	Ga(4)–C(19)	1.988(4)
Ga(2)–N(1)	2.009(3)	Ga(4)–N(2)	2.016(3)
Ga(2)–N(4)	2.012(4)	Ga(4)–N(3)	2.019(4)
Ga(2)–N(5)	1.855(4)	Ga(4)–N(5)	1.855(3)
C(1)–Ga(1)–N(1)	105.81(15)	C(13)–Ga(3)–N(3)	113.95(16)
C(1)–Ga(1)–N(2)	112.56(15)	C(13)–Ga(3)–N(4)	108.42(16)
C(1)–Ga(1)–N(6)	122.92(16)	C(13)–Ga(3)–N(6)	116.13(15)
N(1)–Ga(1)–N(2)	103.84(15)	N(3)–Ga(3)–N(4)	98.45(16)
N(1)–Ga(1)–N(6)	104.83(14)	N(3)–Ga(3)–N(6)	107.88(14)
N(2)–Ga(1)–N(6)	105.09(15)	N(4)–Ga(3)–N(6)	110.60(15)
C(7)–Ga(2)–N(1)	106.09(16)	C(19)–Ga(4)–N(2)	108.11(17)
C(7)–Ga(2)–N(4)	111.69(17)	C(19)–Ga(4)–N(3)	114.82(16)
C(7)–Ga(2)–N(5)	124.45(17)	C(19)–Ga(4)–N(5)	116.19(17)
N(1)–Ga(2)–N(4)	104.41(15)	N(2)–Ga(4)–N(3)	97.85(15)
N(1)–Ga(2)–N(5)	104.21(15)	N(2)–Ga(4)–N(5)	112.12(15)
N(4)–Ga(2)–N(5)	104.17(16)	N(3)–Ga(4)–N(5)	106.31(14)
C(25)–N(1)–Ga(1)	118.6(3)	C(37)–N(4)–Ga(2)	110.1(3)
C(25)–N(1)–Ga(2)	113.4(3)	C(37)–N(4)–Ga(3)	110.5(3)
Ga(1)–N(1)–Ga(2)	119.05(17)	C(37)–N(4)–H(4N)	111(3)
C(29)–N(2)–Ga(1)	110.9(3)	Ga(2)–N(4)–Ga(3)	115.29(17)
C(29)–N(2)–Ga(4)	109.4(2)	Ga(2)–N(4)–H(4N)	104(3)
C(29)–N(2)–H(2N)	111(3)	Ga(3)–N(4)–H(4N)	106(3)
Ga(1)–N(2)–Ga(4)	115.06(17)	C(41)–N(5)–Ga(2)	119.4(3)
Ga(1)–N(2)–H(2N)	107(3)	C(41)–N(5)–Ga(4)	119.4(3)
Ga(4)–N(2)–H(2N)	103(3)	Ga(2)–N(5)–Ga(4)	120.63(18)
C(33)–N(3)–Ga(3)	112.7(3)	C(45)–N(6)–Ga(1)	119.6(3)
C(33)–N(3)–Ga(4)	120.4(4)	C(45)–N(6)–Ga(3)	120.2(3)
Ga(3)–N(3)–Ga(4)	115.39(16)	Ga(1)–N(6)–Ga(3)	120.17(18)

tures, such as $(\text{ClAl})_4(\text{NMe}_2)_4(\text{NMe})_2$,²³ $[\text{Ga}_4\text{S}_{10}]$,^{8–24} $[\text{In}_4\text{S}_{10}]$,^{8–24} $[\text{In}_4\text{Se}_{10}]$,^{8–24} $(\text{IGa})_4(\text{SMe}_4)_2\text{S}_2$,²⁵ and $(\text{IAl})_4$ -

(23) Rhewalt, U.; Kawada, I. *Chem. Ber.* **1970**, *103*, 2754–2769.

(24) Krebs, B.; Voelker, D.; Stiller, K.-O. *Inorg. Chim. Acta* **1982**, *65*, L101–L102.

(22) Luo, B.; Gladfelter, W. L. *J. Chem. Soc., Chem. Commun.* **2000**, 825–826.

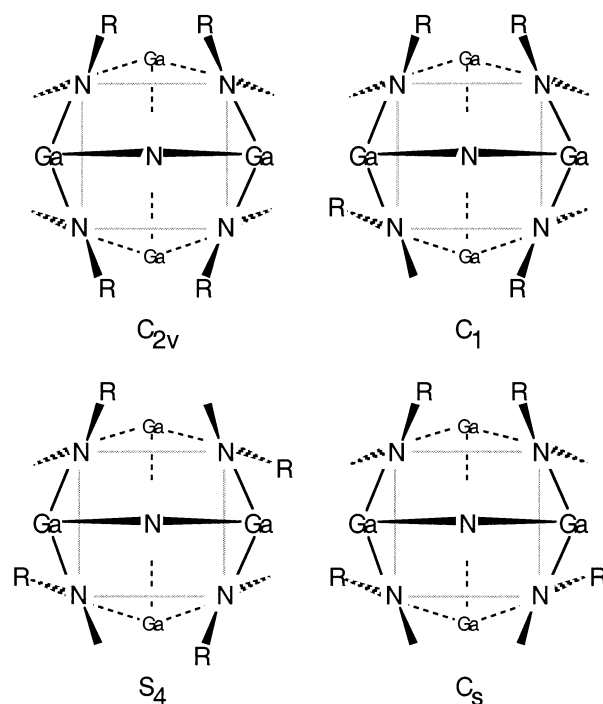
Table 3. Selected Bond Lengths (Å) and Angles (deg) for (PhGa)₇(NHMe)₄(NMe)₅ (2)

Ga(1)–C(1)	1.980(10)	Ga(4)–N(4)	1.984(3)
Ga(1)–N(1)	1.952(4)	Ga(4)–N(5)	1.979(3)
Ga(1)–N(2)	1.985(3)	Ga(5)–C(25)	1.993(6)
Ga(1)–N(3)	1.903(4)	Ga(5)–N(4)	1.961(3)
Ga(2)–C(7)	1.994(4)	Ga(5)–N(8)	1.943(4)
Ga(2)–N(1)	1.955(3)	Ga(5)–N(9)	1.981(4)
Ga(2)–N(4)	1.977(3)	Ga(6)–C(31)	1.986(4)
Ga(2)–N(6)	1.966(3)	Ga(6)–N(6)	1.988(3)
Ga(3)–C(13)	1.984(4)	Ga(6)–N(7)	1.942(3)
Ga(3)–N(2)	1.997(3)	Ga(6)–N(8)	1.946(3)
Ga(3)–N(5)	1.957(3)	Ga(7)–C(37)	1.985(4)
Ga(3)–N(6)	1.957(3)	Ga(7)–N(5)	1.978(3)
Ga(4)–C(19)	2.001(5)	Ga(7)–N(7)	1.906(3)
Ga(4)–N(3)	1.908(3)	Ga(7)–N(9)	1.998(3)

C(1)–Ga(1)–N(1)	108.1(4)	C(43)–N(1)–Ga(1)	112.5(3)
C(1)–Ga(1)–N(2)	108.2(5)	C(43)–N(1)–Ga(2)	117.2(3)
C(1)–Ga(1)–N(3)	125.1(4)	C(43)–N(1)–H(1N)	102.2
N(1)–Ga(1)–N(2)	101.49(14)	Ga(1)–N(1)–Ga(2)	117.29(18)
N(1)–Ga(1)–N(3)	107.07(16)	C(44)–N(2)–Ga(1)	109.5(2)
N(2)–Ga(1)–N(3)	104.38(15)	C(44)–N(2)–Ga(3)	114.0(3)
C(7)–Ga(2)–N(1)	107.32(17)	C(44)–N(2)–H(2N)	105.1
C(7)–Ga(2)–N(4)	113.49(17)	Ga(1)–N(2)–Ga(3)	116.89(16)
C(7)–Ga(2)–N(6)	115.10(15)	C(45)–N(3)–Ga(1)	118.1(3)
N(1)–Ga(2)–N(4)	107.95(15)	C(45)–N(3)–Ga(4)	117.6(3)
N(1)–Ga(2)–N(6)	106.52(14)	Ga(1)–N(3)–Ga(4)	119.29(18)
N(4)–Ga(2)–N(6)	106.07(13)	C(46)–N(4)–Ga(2)	106.3(3)
C(13)–Ga(3)–N(2)	104.12(15)	C(46)–N(4)–Ga(4)	105.7(3)
C(13)–Ga(3)–N(5)	116.76(15)	C(46)–N(4)–Ga(5)	109.0(3)
C(13)–Ga(3)–N(6)	114.99(14)	Ga(2)–N(4)–Ga(4)	112.88(16)
N(2)–Ga(3)–N(5)	107.92(14)	Ga(2)–N(4)–Ga(5)	109.01(16)
N(2)–Ga(3)–N(6)	104.31(13)	Ga(4)–N(4)–Ga(5)	113.59(16)
N(5)–Ga(3)–N(6)	107.73(13)	C(47)–N(5)–Ga(3)	107.3(2)
C(19)–Ga(4)–N(3)	111.88(18)	C(47)–N(5)–Ga(4)	106.2(2)
C(19)–Ga(4)–N(4)	112.09(18)	C(47)–N(5)–Ga(7)	108.8(2)
C(19)–Ga(4)–N(5)	111.39(17)	Ga(3)–N(5)–Ga(4)	112.96(16)
N(3)–Ga(4)–N(4)	108.74(15)	Ga(3)–N(5)–Ga(7)	109.46(15)
N(3)–Ga(4)–N(5)	107.52(14)	Ga(4)–N(5)–Ga(7)	111.91(15)
N(4)–Ga(4)–N(5)	104.88(13)	C(48)–N(6)–Ga(2)	108.6(2)
C(25)–Ga(5)–N(4)	116.4(3)	C(48)–N(6)–Ga(3)	106.8(2)
C(25)–Ga(5)–N(8)	114.1(3)	C(48)–N(6)–Ga(6)	108.1(2)
C(25)–Ga(5)–N(9)	107.4(3)	Ga(2)–N(6)–Ga(3)	113.97(15)
N(4)–Ga(5)–N(8)	107.05(14)	Ga(2)–N(6)–Ga(6)	111.08(15)
N(4)–Ga(5)–N(9)	106.18(15)	Ga(3)–N(6)–Ga(6)	108.09(14)
N(8)–Ga(5)–N(9)	104.86(16)	C(49)–N(7)–Ga(6)	115.7(3)
C(31)–Ga(6)–N(6)	115.17(15)	C(49)–N(7)–Ga(7)	115.7(3)
C(31)–Ga(6)–N(7)	109.97(16)	Ga(6)–N(7)–Ga(7)	119.06(16)
C(31)–Ga(6)–N(8)	114.72(16)	C(50)–N(8)–Ga(5)	114.2(3)
N(6)–Ga(6)–N(7)	106.02(13)	C(50)–N(8)–Ga(6)	114.2(3)
N(6)–Ga(6)–N(8)	104.56(14)	C(50)–N(8)–H(8N)	102.8
N(7)–Ga(6)–N(8)	105.60(15)	Ga(5)–N(8)–Ga(6)	117.29(17)
C(37)–Ga(7)–N(5)	113.91(16)	C(51)–N(9)–Ga(5)	111.5(3)
C(37)–Ga(7)–N(7)	117.02(16)	C(51)–N(9)–Ga(7)	110.1(3)
C(37)–Ga(7)–N(9)	108.10(17)	C(51)–N(9)–H(9N)	106.6
N(5)–Ga(7)–N(7)	105.41(14)	Ga(5)–N(9)–Ga(7)	114.92(17)
N(5)–Ga(7)–N(9)	107.03(14)	N(7)–Ga(7)–N(9)	104.59(15)

(SMe)₄S₂,²⁶ reveals a smaller range of bond angles on the metal. The larger variation for the N–Ga–N bond angles in the structure of **1** is likely attributable to the steric repulsions among the bulky phenyl and isobutyl ligands.

Within the adamantyl framework, the six nitrogens (two imido and four amido ligands) are located at the apexes of an octahedron. The two imido nitrogens, N(5) and N(6), are trans to each other, and the four amido ligands define the equatorial plane. A second isomer in which the imido ligands

**Figure 3.** View down the N(5)–N(6) axis showing the four possible isomers caused by switching the R (ⁱBu) and H substituents on the four amido ligands located in the equatorial plane.

are cis is possible, but this arrangement would require ligation of two imido ligands to one of the galliums and create an uneven charge distribution across the cluster. We suggest this would be less favored. In addition to isomers caused by the arrangement of the imido ligands, the relative placement of the ⁱBu and H on each of the amido ligands leads to four possible isomers. If N(1)–N(4) is defined as the equatorial plane, the isobutyl groups can be above the plane (up), defined as oriented toward N(5), or below (down) (see Figure 3). As the two imido ligands are identical, the all-up and all-down arrangements are equivalent and belong to the *C*_{2v} point group. One unique isomer (*C*₁) forms from three up and one down, and two isomers are feasible for the two-up pattern. Specifically, the alkyls on N(1) and N(3) could be up (*S*₄) or the alkyls on N(1) and N(2) could be up (*C*_s).

In the actual crystal structure, the H and ⁱBu substituents on both N(1) and N(3) are disordered. Examination of the orientation of the ⁱBu substituents on the ordered amido ligands, N(2) and N(4) (one up and one down), rules out the possible existence of the *C*_{2v} isomer in the solid state. Perhaps more difficult to see is that the *S*₄ isomer in which the orientations of the substituents on N(2) and N(4) are both on the same side is also eliminated. This leaves two possible isomers, *C*₁ and *C*_s. Because the crystal symmetry is lower than the molecular symmetry, part of the disorder could be explained by two orientations of the same isomer. A 2-fold rotation of the cluster about the N(1)–N(3) axis would leave all atoms in the molecule unchanged, except for those of the disordered substituents on N(1) and N(3). This orientational disorder within the crystal cannot account for all of the disorder. The refined occupancy factor of the ⁱBu on N(1) in the up position is 0.551 (the down position corresponds to 1 – 0.551 = 0.449). The up orientation also predominates

(25) Boardman, A.; Jeffs, S. E.; Small, R. W. H.; Worrall, I. J. *Inorg. Chim. Acta* **1984**, 83, L39–L40.

(26) Boardman, A.; Small, R. W. H.; Worrall, I. J. *Inorg. Chim. Acta* **1986**, 120, L23–L24.

(occupancy = 0.657) for the i Bu groups attached to N(3). Rotational disorder alone would require that these two numbers be related. Thus, we conclude that the C_s and C_1 isomers coexist in the crystal structure.

The structure of **2**, shown in Figure 2, is unique among gallium–nitrogen clusters and even among the larger number of related aluminum–nitrogen compounds. It consists of three layers. In layer 1 galliums 5–7 and nitrogens 7–9 comprise a six-membered ring in a chair conformation. The middle (second) layer involving galliums 2–4 and nitrogens 4–6 is also in a chair conformation and connected to the first layer by three Ga–N bonds. The top (third) layer is best considered as a capping tripodal ligand in which the three nitrogens of $[\text{PhGa}(\text{NHMe})_2(\text{NMe})]^{2-}$ bond to the galliums in the middle layer.

In addition to the disorder of the solvents of crystallization, the phenyl groups on four of the seven galliums are disordered. On Ga(2) and Ga(4), the phenyl groups exist in two orientations differing by rotation about the Ga–C bond. On Ga(1) and Ga(5) the phenyl is disordered by a slight change in the angular position of gallium-bound carbon such that all carbons in both orientations essentially lie in the same plane.

In the structure of compound **2**, all gallium atoms adopted distorted tetrahedral geometries with each bonded to three nitrogen atoms and one phenyl ligand. Three types of nitrogen atoms were found: the four-coordinate amido ligands [N(1), N(2), N(8) and N(9)]; three-coordinate imido ligands [N(3) and N(7)]; four-coordinate imido ligands [N(4), N(5), and N(6)]. The geometries on the imido nitrogens N(3) and N(7) deviated from planarity as indicated by the sum of the angles among them being 355.0 and 350.5°, respectively. They were recognized as imido ligands on the basis of the significantly shorter bonds of Ga(1)–N(3) [1.903(4) Å], Ga(4)–N(3) [1.908(3) Å], and Ga(7)–N(7) [1.906(3) Å] compared to other Ga–N bonds [1.943(4)–1.998(3) Å] in the structure. The N–Ga–N bond angles ranged from 101.49(14) to 108.74(15)°. The Ga–N–Ga bond angles on the nitrogens bonded to three gallium atoms [108.09(14)–113.97(15)°] were smaller than those bonded to two gallium atoms [114.92(17)–119.29(28)°].

The rigidity of the cluster framework could allow isomers to arise from the H/Me interchange on each of the four amido ligands. In addition, the positions of two of the five imido groups, N(3)–C(45) and N(9)–C(49), could be coplanar, as indicated in the C_s isomer in Figure 4, or nonplanar as in C_1 . The latter corresponds to the solid-state structure.

While this situation could lead to a large number of isomers, consideration of the steric repulsion among the ligands helps to simplify the picture. The methyl substituents on N(8) and N(9) reside in axial positions relative to the six-membered ring comprised of galliums 5–7 and nitrogens 7–9. In both cases, the alternative equatorial position is rendered unfavorable by the presence of the phenyl groups on Ga(2) and Ga(4). Smaller energetic differences should exist for the isomeric configurations of the methyls on N(1) and N(2). We define the methyls on these nitrogens as *exo* or *endo* on the basis of their position relative to the area

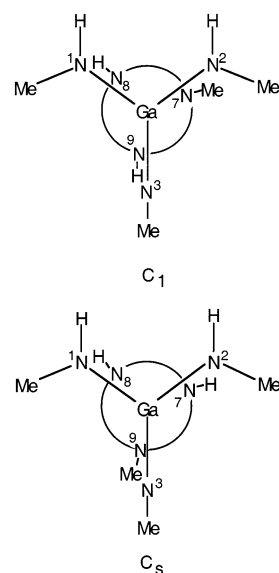


Figure 4. Newman-like projections illustrating two of the isomers of $(\text{PhGa})_7(\text{NMe})_5(\text{NHMe})_4$ (**2**). The atoms of the middle Ga_3N_3 ring are not shown. The isomer labeled C_1 corresponds to that found in the solid-state structure, and the numbers adjacent to the nitrogens refer to that numbering scheme. The methyls on N(1) and N(2) are shown in the *exo* positions.

bordered by rays from N(3) to N(1) and N(3) to N(2). The two structures shown in Figure 4 have all methyls in the *exo* positions. For the unsymmetric C_1 isomer, all four permutations (*exo*–*exo*, *exo*–*endo*, *endo*–*exo*, and *endo*–*endo*) are unique. For the C_s isomer, the *exo*–*endo* and *endo*–*exo* configurations are enantiomeric; thus, only three isomers could be distinguished. From the perspective of steric interactions among the substituents on N(1), N(2), and N(3), the *exo*–*exo* isomer would appear to be most favorable and the *endo*–*endo* isomer would be the least.

Spectroscopic Properties of 1 and 2. The IR spectra exhibited absorptions at 3281 and 3169 cm^{-1} for **1** and 3265 cm^{-1} for **2**, indicating the presence of N–H moieties in both compounds. In the chemical-ionization mass spectrum of compound **1** collected in CH_4 with 4% NH_3 at an evaporation temperature of ca. 310 °C, peaks were found at m/e 1036 for $(\text{M} + \text{NH}_4)^+$, 1014 for $(\text{M} - \text{Ph} + \text{H}_2\text{N}^i\text{Bu})^+$, and 941 for $(\text{M} - \text{Ph})^+$. Several peaks with high intensities, however, were not the direct fragmentation products of compound **1**; the base peak at m/e 873 was assigned to $(\text{PhGaN}^i\text{Bu})_4$, and related ions $\{(\text{PhGaN}^i\text{Bu})_4 + \text{NH}_4\}^+$ and $\{(\text{PhGaN}^i\text{Bu})_4 - \text{Ph}\}^+$ were also present. Peaks attributed to $(\text{Ph}_2\text{GaNH}^i\text{Bu})_2$ (plus 1) and $\{(\text{Ph}_2\text{GaNH}^i\text{Bu})_2 - \text{Ph} + \text{NH}_3\}^+$ were found with the intensities of 4 and 14% of the base peak, respectively. As described below, $(\text{Ph}_2\text{GaNH}^i\text{Bu})_2$ was a pyrolysis product of compound **1**. It was not possible to establish whether $(\text{PhGaN}^i\text{Bu})_4$ formed from the benzene elimination of $(\text{Ph}_2\text{GaNH}^i\text{Bu})_2$ or directly from **1** by elimination of $i\text{BuNH}_2$. In the MS experiment for compound **2** as described in the Experimental Section, two spectra were recorded corresponding to the two maxima in the ion abundance curve. The spectrum corresponding to the evaporation temperature of 340 °C exhibited numerous low-mass peaks (below m/e 450) including the base peak of C_6H_6^+ . Only three peaks were found in the higher mass region. The

peak at m/e 1231 with an intensity of 5.6% of the base peak was assigned to heptameric $(\text{PhGaNMe})_7^+$. The peaks at m/e 1218 and 1154 were assigned to $\{(\text{PhGaNMe})_7 - \text{Me} + 2\text{H}\}^+$ and $\{(\text{PhGaNMe})_7 - \text{Ph}\}^+$, respectively. It was observed during the melting-point measurement that compound **2** decomposed at 173 °C; however, the products of this thermolysis were not characterized.

The room-temperature, 500 MHz ^1H NMR spectrum of compound **1** exhibited a complex pattern; more than 40 overlapping multiplets were found for the N^iBu and NH^iBu ligands. Although the individual methyl (0.2–0.4 ppm), methine (1.4–2.0 ppm), and methylene (2.2–4.0 ppm) regions appear distinct, the overlap and complexity of the splitting patterns within these regions were too great for interpretation. Greater value was derived by examination of the phenyl hydrogens. Two distinct regions located from 6.9 to 7.5 and 7.6 to 8.1 were present with the relative intensity of 3:2, respectively. The downfield resonances consisted of at least 10 doublets typically having coupling constants of 7 Hz and were assigned to the *ortho* hydrogens. With intensities approximately 3 times larger, three of the doublets (located at 7.75, 7.81, and 7.87) dominated this region. The relative intensity among these three was 1:1:2. Two isomers, identified in Figure 3 as C_s and C_1 , cocrystallized in the solid state and could be present in solution. The C_s isomer is the only isomer in Figure 3 that would give rise to a 1:1:2 pattern for the phenyl groups. Four doublets of equivalent intensity at 7.63, 7.95, 7.96, and 8.00 ppm are tentatively assigned to the C_1 isomer. The three remaining, smallest doublets, located at 7.61, 7.70, and 7.78 ppm, may be due to the two phenyl resonances expected for the C_{2v} isomer and the sole doublet of the S_4 isomer. The ^1H NMR spectrum was unchanged in the temperature range from –60 to +95 °C. This lack of temperature dependence of the ^1H NMR spectrum suggests that these exchanges are slow on the NMR time scale.

The ^1H NMR spectrum of compound **2** exhibits phenyl resonances in the range from 6.8 to 8.3 ppm and methyl and N–H resonances between 0.8 and 3.8 ppm. From the numbers of singlets and doublets attributable to methyl groups of methylimido and methylamido ligands, we recognize the existence of isomers in solution. A 2-D (specifically, an HMQC) $^1\text{H}/^{13}\text{C}$ spectrum establishes correlations between the 12 observable ^{13}C resonances appearing from 38 to 42 ppm and the singlets in the proton spectrum appearing from 2.42 to 3.53 ppm. These singlets are assigned to the methylimido ligands. Ignoring the very low intensity resonances, presumably due to small amounts of other isomers, we distinguish 14 resonances due to NMe groups (including one accidentally degenerate pair at 2.65 ppm), 5 of which are approximately twice the intensity of the others. On the basis of the solid-state structure, the predominant C_1 isomer (referred to as the *exo–exo* C_1 isomer) would yield five NMe resonances with equal intensity. Although none of these assignments can be considered unambiguous, we suggest that the remaining 10 resonances are due to the *endo–exo* and *exo–endo* C_1 isomers.

Three isomers in a 2:1:1 ratio would require the presence of 12 doublets and quartets due to the 4 nonequivalent

methylamido ligands on each isomer. The ^{13}C resonances of the amido ligands are grouped tightly between 32 and 34 ppm (12 observable peaks), and these resonances correlate with the ^1H peaks located between 1.91 and 2.41 ppm. The NH quartets appear over a wider range (0.87–2.70 ppm), and a 2-D COSY experiment was needed to locate some of the resonances and assign the coupling. Even with the aid of an 800 MHz spectrometer, however, substantial overlapping of signals precluded observation of every resonance. A total of 10 NHCH_3 quartets and 11 NHCH_3 doublets were identified, but we were unable to assign these to specific isomers. The above assignments compare favorably to those reported for the ^{13}C resonances of the amido and imido ligands in $(\text{MeGaNHR})_2$ and $(\text{MeGaNR})_4$, where $\text{R} = ^i\text{Pr}$ and ^iBu .¹⁵

Pyrolysis of Compound 1. When a crystalline sample of compound **1** was heated at 150 °C for 2 h, pentane, toluene, and isobutylamine were found to be the major components of the trapped volatiles confirming that the solvents present in the crystals were pentane and toluene. The dimer $(\text{Ph}_2\text{GaNH}^i\text{Bu})_2$ was one of the nonvolatile products. The residual product(s) formed a glassy solid mixture whose ^1H NMR spectrum showed a complex pattern. Pyrolysis of **1** at 300 °C resulted in formation of gallium metal as a product.

Reactions of $[\text{PhGa}(\text{NMe}_2)_2]_2$ with $\text{H}_2\text{N}^i\text{Bu}$ and H_2NMe at Elevated Temperatures. In an attempt to induce further elimination of H_2NR from compounds **1** and **2** to prepare the $(\text{RGaNR}')_n$ type of compounds, reactions were conducted at elevated temperatures. The reaction of $[\text{PhGa}(\text{NMe}_2)_2]_2$ in refluxing $\text{H}_2\text{N}^i\text{Bu}$ (85 °C) gave $(\text{Ph}_2\text{GaNH}^i\text{Bu})_2$ (35% yield based on gallium) as one of the products and an uncharacterized viscous oil (Scheme 1). The formation of $(\text{Ph}_2\text{GaNH}^i\text{Bu})_2$ was consistent with the results from the pyrolysis of compound **1** and indicated a ligand redistribution pathway. The reaction of $[\text{PhGa}(\text{NMe}_2)_2]_2$ with H_2NMe at 150 °C afforded compound **2** in ca. 9% yield. Other products were not characterized.

Discussion

The goal of this study was to explore the impact of intramolecular steric forces on the nuclearity of gallium nitrogen clusters. Specifically, we sought to use nonbonded contacts among ligands on the framework gallium and nitrogen atoms to control the size of the resulting structure. Large ligands have been widely used to produce isolable, unsaturated complexes that are prevented from further reaction by nonbonded repulsive forces. Within group 13 nitrogen chemistry, several such examples, including a dimeric iminoalane with a Al_2N_2 ring²⁷ and $[\text{MeAlN}(2,6\text{-}^i\text{Pr}_2\text{C}_6\text{H}_3)]_3$,²⁸ demonstrate this approach.

The systematic synthetic approach to the hydrocarbylgallium complexes developed in this study was based on chemistry observed during the conversion of $[\text{H}_2\text{GaNH}_2]_3$

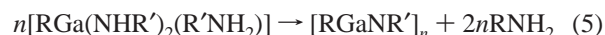
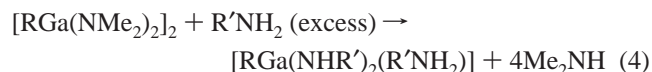
(27) Schulz, S.; Häming, L.; Herbst-Irmer, R.; Roeksy, H. W.; Sheldrick, G. M. *Angew. Chem., Int. Ed. Engl.* **1994**, *33*, 969–970.

(28) Waggoner, K. M.; Hope, H.; Power, P. P. *Angew. Chem., Int. Ed. Engl.* **1988**, *27*, 1699–1700.

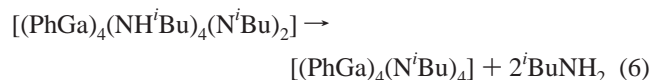
into [HGaNH] in the presence of donors (eqs 1–3).²⁹ The third step in this sequence involved elimination of NH₃ to form imidogallane, [HGaNH].



The recently reported synthesis of hydrocarbylgallium dimethylamides, $[\text{RGa}(\text{NMe}_2)_2]_2$,²¹ provided the necessary starting complexes to synthesize molecules with the general formula $[\text{RGa}(\text{NHR}')_2]$ via the substitution reaction shown in eq 4. As reported in other examples,⁴ loss of gaseous dimethylamine helps to drive the equilibrium represented in eq 4 in the forward direction.



In analogy to eq 3, complete elimination of two molecules of the primary amine, eq 5, would lead to the fully substituted analogue to [HGaNH] in a sequence that would allow systematic variation of both R and R'. The high-yield preparations of $(\text{XIn}^i\text{NBu})_4$ (X = Cl, Br, and I) from the reactions of InX_3 and 2 equiv of LiNH^iBu have proven the success of this type of reaction in indium chemistry.³⁰ In the current study methylamine and isobutylamine were reacted with $[\text{PhGa}(\text{NMe}_2)_2]_2$ under a variety of conditions, and the products isolated from these reactions were consistent with the concept that ligand size can influence the nuclearity. The larger isobutylamine produced the smaller, tetragallium cluster, while a heptagallium complex was formed in the reaction with methylamine. The chemistry, however, was more complicated than suggested by eq 5. Instead of undergoing complete alkylamine elimination, the products isolated, **1** and **2**, retained some of the alkylamido ligands (Scheme 1). Attempts to force the reaction to completion by pyrolysis, eq 6, instead resulted in ligand redistribution reactions leading to low yields of $[\text{Ph}_2\text{Ga}(\text{NH}^i\text{Bu})]_2$ or at still higher temperatures to the formation of metallic gallium.



It was interesting that the most intense ion in the mass spectrum of **1** did indeed correspond to the formula, $[(\text{PhGa})_4(\text{N}^i\text{Bu})_4]$, of the cubane cluster, and $[(\text{PhGa})_7(\text{NMe})_7]$ and related ion peaks were the only high-mass peaks in the spectrum of **2**. It was not possible to determine whether these

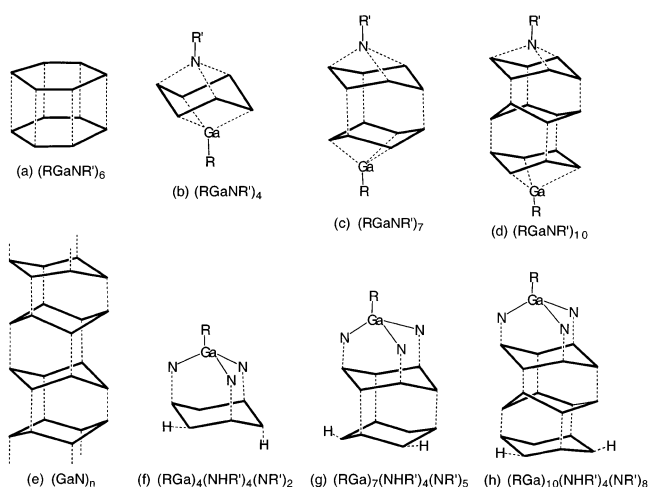


Figure 5. Relationship among the gallium imido clusters (a–d), gallium amido imido clusters (f–h), and hexagonal GaN (e). Each six-membered ring represents a Ga_3N_3 unit.

were due to gas-phase fragmentation before or after ionization or to pyrolysis in the probe.

Structures of Gallium Imido and Gallium Amido Imido Clusters. An alternative approach to gallium imido clusters involves hydrocarbon elimination from complexes with the general formula $[\text{R}_2\text{GaNHR}']$. Both $[(\text{PhGa})_4(\text{NPh})_4]$ and $[(\text{PhGa})_7(\text{NMe})_7]$ were synthesized recently by this route¹³ and follow the pattern of larger substituents leading to lower nuclearities. The structural relationship among these two gallium imido clusters, hexameric prismatic structures, higher oligomers, and the solid-state structure of hexagonal GaN was discussed¹³ and is represented in Figure 5a–e. The gallazine ring $(\text{RGa})_3(\text{NR}')_3$ is highlighted as being the common building block. In $[(\text{PhGa})_4(\text{NPh})_4]$ and $[(\text{PhGa})_7(\text{NMe})_7]$ saturation of the coordination spheres of gallium at one end of the cluster is accomplished with an $\text{R}'\text{N}^{2-}$ ligand. Charge compensation occurs at the other end of the cluster by coordination of an RGa^{2+} moiety to the three imido nitrogens.

A similar argument can be applied to understand the structures of the amido–imido clusters produced in this publication. As Figure 5f suggests, if we identify a gallazine ring, $[(\text{PhGa})_3(\text{N}^i\text{Bu})_3]$, as the core of the structure in **1**, the three galliums of this ring can achieve saturation by complexation to a capping tripodal ligand, $[(\text{PhGa})(\text{NH}^i\text{Bu})_2(\text{N}^i\text{Bu})]^{2-}$. The negative charge can be conveniently balanced by adding protons to two of the imido ligands of the cluster. Two chair-shaped gallazine rings joined by three Ga–N bonds comprise the core of **2**. Figure 5g illustrates that the top of the two-ring unit is capped by the $[(\text{PhGa})(\text{NHMe})_2(\text{NMe})]^{2-}$ unit and that the charge is balanced by converting two three-coordinate imido ligands into four-coordinate amido ligands by protonation.

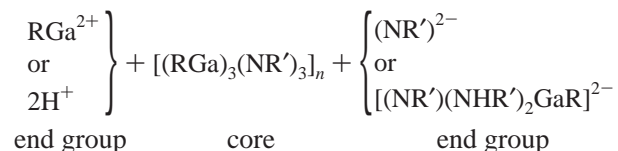
Can this pattern be extended to larger oligomers or polymers? The next higher oligomer in this series is shown in Figure 5h. The answer clearly depends on the size of the substituents both on gallium and nitrogen. In **2** both the amido and imido methyls are in axial positions. If another Ga_3N_3 layer was added below this plane the methyls on N(7)

(29) Jegier, J. A.; Mckernan, S.; Gladfelter, W. L. *Inorg. Chem.* **1999**, *38*, 2726–2733.

(30) Grabowy, Th.; Merzweiler, K. Z. *Anorg. Allg. Chem.* **2000**, *626*, 736–740.

to N(9) would be forced into the equatorial positions (referring to the plane that is perpendicular to the long axis of the cluster). This would increase the amount of steric congestion with the phenyl groups on the gallium in the next plane [e.g. N(9) and Ga(4)]. Smaller substituents on either or both the galliums and nitrogens would facilitate the formation of oligomers or polymers.

Further generalization would allow combinations from either set of end groups thus far identified in these studies:



Attempts to extend this to larger clusters are underway.

Acknowledgment. The authors gratefully acknowledge support from the National Science Foundation. We also thank Drs. Victor G. Young and Maren Pink for their assistance with the single-crystal XRD experiments. The 800 MHz NMR instrumentation was purchased with funds from the NSF (Grant BIR-961477), the University of Minnesota Medical School, and the Minnesota Medical Foundation. We thank Dr. Letitia Yao for obtaining the 800 MHz spectra and assisting with their analysis.

Supporting Information Available: X-ray crystallographic files in CIF format for the structure determinations of compounds **1** and **2** and the ^1H NMR spectra for compounds **1** and **2**. This material is available free of charge via the Internet at <http://pubs.acs.org>.

IC020093G